

Computational Modelling of Point Defects in Lithium Garnets

Alexander G. Squires^{†*}, Alison Walker[‡] & Benjamin J. Morgan[†]

[†]Department of Chemistry, University of Bath, Bath, BA2 7AX

[‡]Department of Physics, University of Bath, Bath, BA2 7AY

*a.g.squires@bath.ac.uk



EPSRC

Engineering and Physical Sciences
Research Council

Introduction

Lithium garnets are promising solid electrolytes for all-solid-state Li ion batteries. In this work, we consider $\text{Li}_7\text{La}_3\text{Zr}_2\text{O}_{12}$ (LLZO) as a model Li-garnet. Dependant on dopants, LLZO has reported room temperature Li conductivity of 10^{-3} to 10^{-4} S cm^{-1} .^{1,2} Recently Kuibek et al. posited that the lattice of LLZO could accommodate O vacancies.³ By elastically deforming the LLZO lattice, O vacancies can impact phase formation and stabilisation; any lattice deformations could also affect the migration barriers and conduction paths of Li ions. Furthermore, if these O vacancies are mobile, conductivity measurements may erroneously conflate O and Li diffusion. Also of interest is the degradation of the LLZO owing to H/Li exchange during synthesis,⁴ followed by subsequent reaction when exposed to atmospheric CO_2 .^{5,6} If the conditions under which this exchange readily takes place can be understood, then it can be minimised during synthesis.

We are interested in calculating charge-dependent formation energies for Li interstitials and vacancies, O vacancies, and interstitial H in both the tetragonal and cubic phases of LLZO using DFT methods to aid in the understanding of the theoretical basis from which these observations arise. The work presented here concerns the tetragonal phase of LLZO, the structure of which is presented in Figure 1. Figures 2 and 3 concern the structural differences between the ordered tetragonal phase and the disordered cubic phase detailing the unique lattice sites considered in this work.

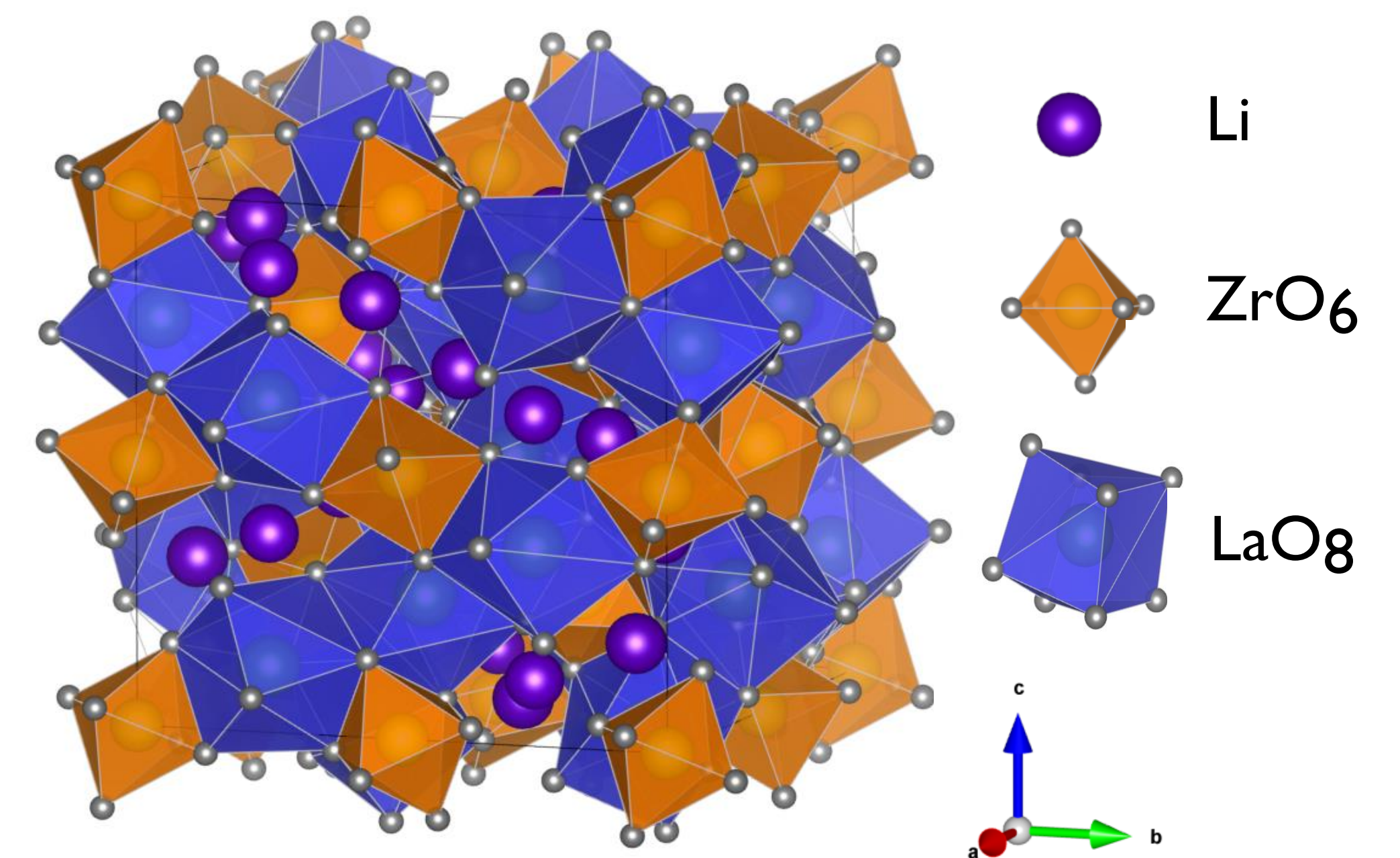


Figure 1. The structure of tetragonal LLZO showing dodecahedral LaO_8 , octahedral ZrO_6 , and the positions of the Li ions.⁷

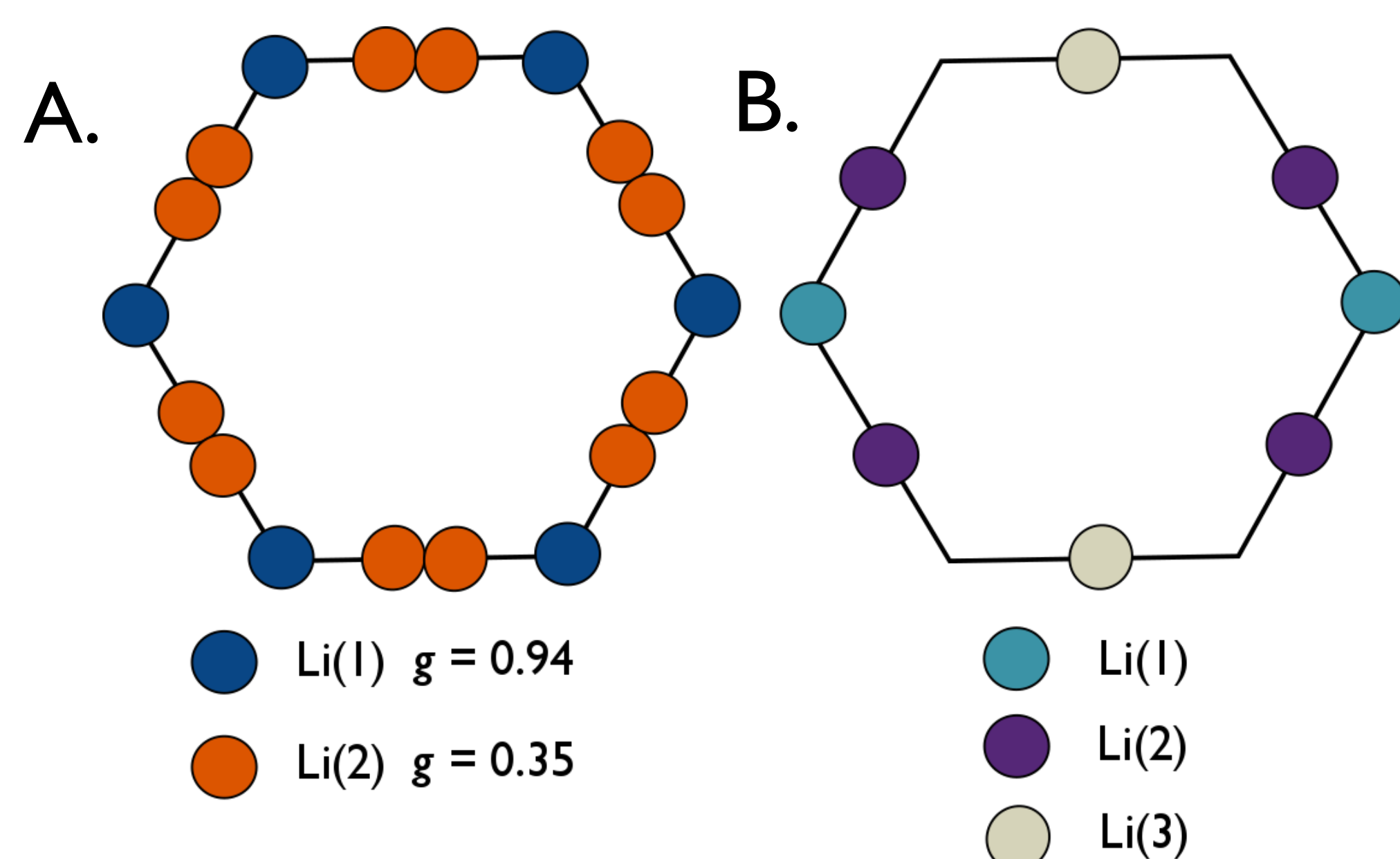


Figure 2. Li arrangement in (A) cubic and (B) tetragonal phase LLZO. Occupancies (g) are given for the cubic phase.⁸ These schematics show the rings that comprise the Li diffusion network for the two phases, ions on the vertices of the rings are tetrahedrally coordinated to O ions, and ions on the edges are octahedrally coordinated. In the tetragonal phase, these are the sites that have been investigated for both Li vacancies, and H substitution.

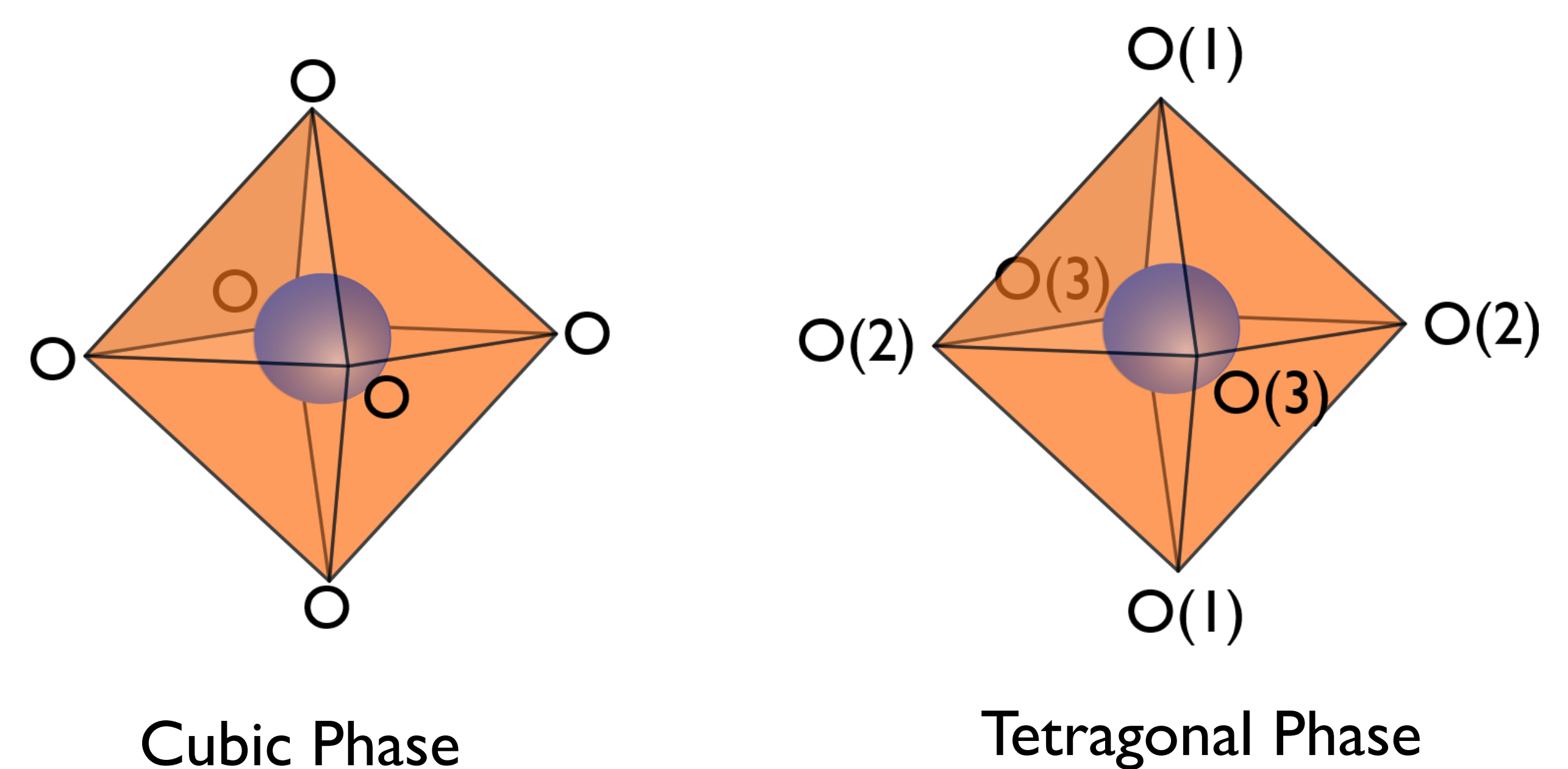


Figure 3. ZrO_6 octahedron in the both phases of the garnet, with O ions shown on the vertices of the octahedron, and Zr shown in blue. In the cubic structure, all O ions are symmetrically equivalent.; on imposition of tetragonal distortion, three separate O sites are created, and are labelled as such on the tetragonal phase distorted octahedra.

Results and discussion

Figure 4 shows formation energies with respect to Fermi level for a range of defects in LLZO. Examining these energies suggests compensation between $V_{\text{O}}^{\bullet\bullet}$ and V_{Li}' with the Fermi level at ~ 1.4 eV. This offers a relatively low energy process by which O vacancies can form as compared to V_{O}^{\times} (~ 3 eV vs 6.25 eV). This suggests that O vacancies could be feasible in LLZO in the form of $V_{\text{O}}^{\bullet\bullet}$, as suggested in ref 3.

Also shown is the H/Li substitution energy. It is apparent that V_{Li}^{\times} is a higher energy species than $\text{H}_{\text{Li}}^{\times}$; suggesting that H will incorporate readily into the lattice of these materials. These results going forward will allow us to calculate equilibrium defect concentrations as a function of synthesis conditions, and hopefully aid in the design of synthesis conditions that will minimise future degradation of the garnet under atmospheric conditions, it will also be interesting to investigate how the presence of O vacancies effect Li conduction properties in LLZO.

References

- [1] Thangadurai, V.; Narayanan, S.; Pinzaru, D. *Chem. Soc. Rev.* **2014**, 43 (13), 4714.
- [2] Chen, R.; Qu, W.; Guo, X.; Li, L.; Wu, F. *Mater. Horiz.* **2016**, 3 (6), 487–516.
- [3] Kubicek, M.; Wachter-Welzl, A.; Rettenwander, D.; Wagner, R.; Berendts, S.; Uecker, R.; Amthauer, G.; Hutter, H.; Fleig, J. *Chem. Mater.* **2017**, 29 (17), 7189–7196.
- [4] Bernuy-Lopez, C.; Manalastas, W.; Lopez Del Amo, J. M.; Aguadero, A.; Aguesse, F.; Kilner, *Chem. Mater.* **2014**, 26 (12), 3610–3617.
- [5] Galven, C.; Fourquet, J. L.; Crosnier-Lopez, M. P.; Le Berre, F. *Chem. Mater.* **2011**, 23 (7), 1892–1900.
- [6] Rustad, J. R. *arXiv.org, e-Print Arch., Condens. Matter* **2016**, 1–9.
- [7] Awaka, J.; Kijima, N.; Hayakawa, H.; Akimoto, J. *J. Solid State Chem.* **2009**, 182 (8), 2046–2052.
- [8] Awaka, J.; Takashima, A.; Kataoka, K.; Kijima, N.; Idemoto, Y.; Akimoto, J. *C. Chem. Lett.* **2011**, 40 (1), 60–62.
- [9] Perdew, J.; Ruzsinszky, A.; Csonka, G.; Vydrov, O.; Scuseria, G.; Constantin, L.; Zhou, X.; Burke, K. *Phys. Rev. Lett.* **2008**, 100 (13), 136406.
- [10] Jain, A.; Ong, S. P.; Hautier, G.; Chen, W.; Richards, W. D.; Dacek, S.; Cholia, S.; Gunter, D.; Skinner, D.; Ceder, G.; Persson, K. A. *APL Mater.* **2013**, 1 (1).
- [11] Fletcher, D. A.; McMeeking, R. F.; Parkin, D. J. *Chem. Inf. Comput. Sci.* **1996**, 36, 746–749.

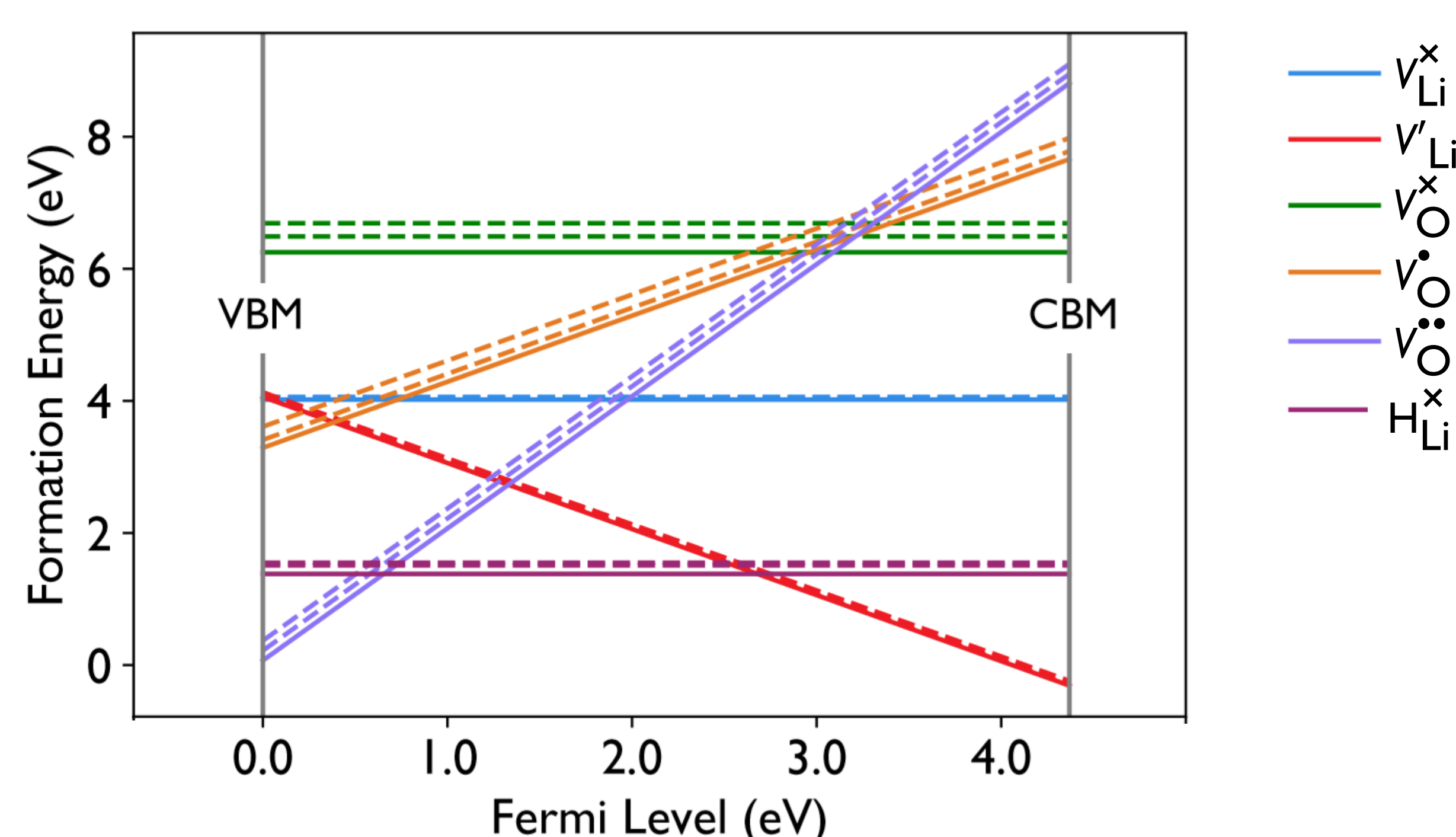


Figure 4. Calculated vacancy defect formation energies in tetragonal LLZO. Defects are represented in the legend using Kröger-Vink notation. The range of Fermi energies presented correspond to the bandgap, where $E_f = 0$ represents the VBM. All potential sites for each defect have been investigated, with the lowest energy site represented with a solid line, other energies represented with a dashed line.

Methodology

- Density Functional Theory calculations implemented in VASP.
- 520 eV plane wave energy cut-off
- $3 \times 3 \times 3$ Monkhorst-Pack k -point grid
- Structural Relaxation to 0.01 eV \AA^{-1}
- Electronic Relaxation to 10^{-4} eV
- PBEsol GGA XC-functional used⁹
- Input structural data taken from a combination of the Materials Project (MP)¹⁰ and the Inorganic Crystal Structure Database (ICSD).¹¹